

HIGH ACCURACY RECONSTRUCTION FROM WAVELET COEFFICIENTS

FRITZ KEINERT AND SOON-GEOL KWON

ABSTRACT. The accuracy of the wavelet approximation at resolution $h = 2^{-n}$ to a smooth function f is limited by $O(h^N)$, where N is the number of vanishing moments of the mother wavelet ψ . For any positive integer p , we derive a new approximation formula which allows us to recover a smooth f from its wavelet coefficients with accuracy $O(h^p)$. Related formulas for recovering derivatives of f are also given.

1. INTRODUCTION

Let $\phi, \tilde{\phi}$ be the scaling functions of a biorthogonal multiresolution approximation. The projection

$$\tilde{P}_n f = \sum_{j=-\infty}^{\infty} \langle f, \phi_{n,j} \rangle \tilde{\phi}_{n,j} \quad (1.1)$$

of a function $f \in L^2(\mathbb{R})$ onto the space \tilde{V}_n spanned by

$$\tilde{\phi}_{n,k}(x) = 2^{n/2} \tilde{\phi}(2^n x - k), \quad k \in \mathbb{Z}, \quad (1.2)$$

is interpreted as an approximation to f at resolution $h = 2^{-n}$. Such projections form the starting point and/or result of any numerical method based on wavelets, from signal processing to wavelet-Galerkin methods.

In practice, the connection between point values of the smooth original function f and its scaling function coefficients is often established by simple formulas such as

$$f_{n,j} = \langle f, \phi_{n,j} \rangle \approx 2^{-n/2} f((j + \tau)h),$$

where $\tau = \int x \phi(x) dx$ is the center of mass of ϕ . For many applications, this is perfectly adequate.

Higher accuracy formulas for the computation of $f_{n,j}$ have been published (see e.g. [6]), but the problem of recovering accurate point values of f from its coefficients $f_{n,j}$ has not received much attention.

It is well-known that if the wavelet ψ has N vanishing moments and f belongs to C^N , then

$$|f(x) - \tilde{P}_n f(x)| = O(h^N).$$

In some applications, such as wavelet-Galerkin methods, we may know the coefficients of a smooth solution function to high accuracy. How do we recover point values of f , and possibly some derivatives of f , to comparable accuracy?

Date: March 21, 1997.

1991 Mathematics Subject Classification. 42C15.

Key words and phrases. wavelets.

For any given scaling function ϕ and accuracy p , we find in this paper a function β with support in an interval of length p so that for smooth f ,

$$|f(x) - \sum_j \langle f, \phi_{n,j} \rangle \beta_{n,j}(x)| = O(h^p), \quad (1.3)$$

where $\beta_{n,j} = 2^{n/2} \beta(2^n x - k)$, $k \in \mathbb{Z}$, in analogy to (1.2). Related functions $\beta^{[r]}$ can be constructed to recover the r th derivative of f to accuracy $O(h^{p-r})$, for any $r < p$.

While the series in (1.3) looks similar to a scaling function expansion, β and $\beta^{[r]}$ do not satisfy any recursion relations in general.

Numerical experiments indicate that our alternative reconstruction formulas perform significantly better than the standard scaling function series (1.1) for smooth f , and are no worse for highly oscillating or non-smooth f . In addition, the new approach allows the reconstruction of derivatives of f .

2. WAVELET BASICS

The fundamentals of wavelet theory have been described in many publications, so we refer to the literature for most of the background, and only introduce the specific notation and results we need. A standard reference for wavelets is [3]. Biorthogonal wavelets are discussed in more detail in [2]. Throughout this paper, we will be using biorthogonal wavelets, which include orthogonal wavelets as a special case.

$L^2(\mathbb{R})$ is the space of square integrable complex-valued functions on \mathbb{R} with inner product

$$\langle f, g \rangle = \int_{\mathbb{R}} f(x) \overline{g(x)} dx,$$

where the bar denotes complex conjugation. ℓ_2 is the space of square summable complex-valued sequences with inner product

$$\langle x, y \rangle = \sum_{i=-\infty}^{\infty} x_i \overline{y_i}.$$

C^r is the space of r times continuously differentiable functions on \mathbb{R} .

A *multiresolution analysis* (MRA) [5] of $L^2(\mathbb{R})$ is a sequence $\{V_j\}_{j \in \mathbb{Z}}$ of closed subspaces of $L^2(\mathbb{R})$ with the properties

- $V_j \subset V_{j+1}$
- $\bigcup_{j=-\infty}^{\infty} V_j$ is dense in $L^2(\mathbb{R})$, and $\bigcap_{j=-\infty}^{\infty} V_j = \{0\}$
- $f(x) \in V_j \iff f(2x) \in V_{j+1}$
- $f(x) \in V_j \iff f(x - 2^{-j}k) \in V_j$ for all $k \in \mathbb{Z}$
- there exists a *scaling function* $\phi(x) \in V_0$ such that the set of translates $\{\phi(x - k)\}_{k \in \mathbb{Z}}$ forms a Riesz basis of V_0 .

Let W_0 be a complement of V_0 in V_1 , that is

$$V_1 = V_0 + W_0.$$

A function $\psi(x) \in W_0$ whose translates $\{\psi(x - k)\}_{k \in \mathbb{Z}}$ form a Riesz basis of W_0 is called a *mother wavelet*. We assume that such a function exists.

Since V_0, W_0 are both subspaces of V_1 , *recursion relations*

$$\begin{aligned}\phi(x) &= \sqrt{2} \sum_k h_k \phi(2x - k), \\ \psi(x) &= \sqrt{2} \sum_k g_k \phi(2x - k),\end{aligned}\tag{2.1}$$

must hold for some sequences $\{h_k\}, \{g_k\}$ in ℓ_2 .

We denote the scaled translates of ϕ, ψ by

$$\begin{aligned}\phi_{n,k}(x) &= 2^{n/2} \phi(2^n x - k), \\ \psi_{n,k}(x) &= 2^{n/2} \psi(2^n x - k).\end{aligned}\tag{2.2}$$

Biorthogonal wavelets are defined by two MRAs of $L^2(\mathbb{R})$, denoted by $\{V_j\}$ and $\{\tilde{V}_j\}$, whose basis functions satisfy the *biorthogonality relations*

$$\begin{aligned}\langle \phi_{n,j}, \tilde{\phi}_{n,k} \rangle &= \delta_{jk}, \\ \langle \psi_{n,j}, \tilde{\psi}_{n,k} \rangle &= \delta_{jk}, \\ \langle \phi_{n,j}, \tilde{\psi}_{n,k} \rangle &= \langle \psi_{n,j}, \tilde{\phi}_{n,k} \rangle = 0.\end{aligned}\tag{2.3}$$

Here δ_{jk} is the Kronecker delta

$$\delta_{jk} = \begin{cases} 0 & \text{if } j \neq k, \\ 1 & \text{if } j = k. \end{cases}$$

For any function $f \in L^2(\mathbb{R})$, projections $P_n f, Q_n f, \tilde{P}_n f, \tilde{Q}_n f$ of f onto $V_n, W_n, \tilde{V}_n, \tilde{W}_n$, respectively, are given by

$$\begin{aligned}P_n f &= \sum_{j=-\infty}^{\infty} \langle f, \tilde{\phi}_{n,j} \rangle \phi_{n,j}, & \tilde{P}_n f &= \sum_{j=-\infty}^{\infty} \langle f, \phi_{n,j} \rangle \tilde{\phi}_{n,j}, \\ Q_n f &= \sum_{j=-\infty}^{\infty} \langle f, \tilde{\psi}_{n,j} \rangle \psi_{n,j}, & \tilde{Q}_n f &= \sum_{j=-\infty}^{\infty} \langle f, \psi_{n,j} \rangle \tilde{\psi}_{n,j}.\end{aligned}$$

In many applications, $P_n f$ and $\tilde{P}_n f$ are interpreted as approximations to f at resolution $h = 2^{-n}$, while $Q_n f$ and $\tilde{Q}_n f$ represent the fine detail in f at resolution h .

The relationship between $\{V_n\}, \{\tilde{V}_n\}$ etc. is completely symmetric. To any definition or algorithm there is a dual, with the tildes in opposite places. We choose to work with \tilde{P}_n instead of P_n in the following sections because it keeps the notation simpler.

The *moments* of $\phi, \psi, \tilde{\phi}, \tilde{\psi}$ are defined as

$$\begin{aligned}\mathcal{M}_i &= \int x^i \phi(x) dx, & \tilde{\mathcal{M}}_i &= \int x^i \tilde{\phi}(x) dx, \\ \mathcal{N}_i &= \int x^i \psi(x) dx, & \tilde{\mathcal{N}}_i &= \int x^i \tilde{\psi}(x) dx.\end{aligned}\tag{2.4}$$

We assume that the scaling functions have been normalized so that $\mathcal{M}_0 = \tilde{\mathcal{M}}_0 = 1$. We say that ψ has N vanishing moments if $\mathcal{N}_0 = \mathcal{N}_1 = \dots = \mathcal{N}_{N-1} = 0, \mathcal{N}_N \neq 0$.

For later use, we also define the *shifted moments* of ϕ

$$\mathcal{M}_{i,j} = \int x^i \phi(x-j) dx = \int (x+j)^i \phi(x) dx = \sum_{s=0}^i \binom{i}{s} j^s \mathcal{M}_{i-s}. \quad (2.5)$$

It is easy to verify that

$$\mathcal{M}_{k,j+1} = \sum_{\ell=0}^k \binom{k}{\ell} \mathcal{M}_{\ell,j}. \quad (2.6)$$

3. CONSTRUCTION OF ALTERNATIVE RECONSTRUCTION FORMULAS

Assume that for some function f and for some biorthogonal wavelet basis we know the projection $\tilde{P}_n f$ onto \tilde{V}_n

$$\tilde{P}_n f = \sum_{j=-\infty}^{\infty} f_{n,j} \tilde{\phi}_{n,j}, \quad (3.1)$$

where

$$f_{n,j} = \langle f, \phi_{n,j} \rangle.$$

How well can we recover the point values of f from this?

Assume that ψ has N vanishing moments. If $f \in C^N$, it is well known and easy to prove that for any point x ,

$$|f(x) - \tilde{P}_n f(x)| = O(h^N),$$

where $h = 2^{-n}$. (See e.g. [6], eq. (1.11); note that the meaning of N , \tilde{N} is reversed compared to our paper).

There are more detailed results available about the convergence rate of $\tilde{P}_n f$ to f under various conditions of f and ϕ (see for example Walter [7], Kelly et al. [4]), but they are all based on the original scaling function series (3.1).

We propose instead to use a different series

$$B_n f = \sum_{j=-\infty}^{\infty} f_{n,j} \beta_{n,j}, \quad (3.2)$$

where

$$\beta_{n,j}(x) = 2^{n/2} \beta(2^n x - j) \quad (3.3)$$

in analogy to (2.2). For any choice of ϕ and for any $p \in \mathbb{N}$, we will produce a function $\beta(x)$ with support of length p so that for $f \in C^p$,

$$|f(x) - B_n f(x)| = O(h^p). \quad (3.4)$$

For simplicity, the dependence of β on p and ϕ is not usually expressed in the notation. If necessary we will write $\beta(x; p)$, and similarly for dependence on other parameters.

More generally, we want to find functions $\beta^{[r]}$ so that

$$|f^{(r)}(x) - B_n^{[r]} f(x)| = O(h^{p-r}), \quad (3.5)$$

where

$$\begin{aligned} f^{(r)} &= \frac{d^r}{dx^r} f, \\ B_n^{[r]} f &= \sum_{j=-\infty}^{\infty} f_{n,j} \beta_{n,j}^{[r]}, \\ \beta_{n,j}^{[r]}(x) &= 2^{n/2} \beta^{[r]}(2^n x - j). \end{aligned} \tag{3.6}$$

To construct β , fix a scaling function ϕ and integers n , p and assume that we are given the scaling function coefficients $f_{n,j}$, $j = 0, \dots, p-1$. Following a standard approach from numerical analysis, we first attempt to find coefficients $c_{n,j}(x)$, $j = 0, \dots, p-1$, so that

$$f(x) = \sum_{j=0}^{p-1} f_{n,j} c_{n,j}(x) \quad \text{for } f(x) = x^k, \quad k = 0, \dots, p-1. \tag{3.7}$$

For $f(x) = x^k$,

$$f_{n,j} = \langle f, \phi_{n,j} \rangle = \int x^k 2^{n/2} \phi(2^n x - j) dx = h^{k+(1/2)} \mathcal{M}_{k,j}.$$

Eq. (3.7) leads to a system of linear equations

$$\mathbf{H}_n \mathbf{M} \mathbf{c}_n(x) = \mathbf{p}(x), \tag{3.8}$$

where

$$\begin{aligned} \mathbf{H}_n &= \mathbf{H}_n(p) = h^{1/2} \begin{pmatrix} h^0 & & & 0 \\ & h^1 & & \\ & & \ddots & \\ 0 & & & h^{p-1} \end{pmatrix}, \\ \mathbf{M} &= \mathbf{M}(\phi, p) = \begin{pmatrix} \mathcal{M}_{0,0} & \mathcal{M}_{0,1} & \cdots & \mathcal{M}_{0,p-1} \\ \mathcal{M}_{1,0} & \mathcal{M}_{1,1} & \cdots & \mathcal{M}_{1,p-1} \\ \vdots & \vdots & \ddots & \vdots \\ \mathcal{M}_{p-1,0} & \mathcal{M}_{p-1,1} & \cdots & \mathcal{M}_{p-1,p-1} \end{pmatrix}, \\ \mathbf{c}_n(x) &= \mathbf{c}_n(x; \phi, p) = \begin{pmatrix} c_{n,0}(x) \\ c_{n,1}(x) \\ \vdots \\ c_{n,p-1}(x) \end{pmatrix}, \\ \mathbf{p}(x) &= \mathbf{p}(x; p) = \begin{pmatrix} x^0 \\ x^1 \\ \vdots \\ x^{p-1} \end{pmatrix}. \end{aligned}$$

It is easy to show that the matrix $\mathbf{M}(\phi, p)$ is nonsingular for all choices of ϕ , p . From definition (2.5), it follows immediately that $\mathbf{M} = \mathbf{B} \cdot \mathbf{V}$, where \mathbf{B} is the lower triangular matrix with entries

$$b_{is} = \binom{i}{s} \mathcal{M}_{i-s}, \quad 0 \leq s \leq i,$$

and \mathbf{V} is the Vandermonde matrix with entries $v_{sj} = j^s$. Hence,

$$\det(\mathbf{M}) = \det(\mathbf{B}) \cdot \det(\mathbf{V}) = \mathcal{M}_0^p \left(\prod_{k=1}^{n-1} k! \right) \neq 0.$$

From

$$\mathbf{c}_n(x) = \mathbf{M}^{-1} \mathbf{H}_n^{-1} \mathbf{p}(x) = h^{-1/2} \mathbf{M}^{-1} \mathbf{p}(x/h),$$

we observe that each $c_{n,j}(x)$ is a polynomial of degree at most $(p-1)$ in (x/h) , and that

$$c_{n,j}(x) = h^{-1/2} c_{0,j}(x/h) = 2^{n/2} c_{0,j}(2^n x). \quad (3.9)$$

To put this approach into a wavelet-like setting, we select a unit interval $I = [x_0, x_0 + 1)$ for some (as yet undetermined) point x_0 . Scaled and shifted versions of I are denoted by $I_{n,s} = [(x_0 + s)h, (x_0 + s + 1)h)$.

We restrict the use of formula (3.7) to the interval $I_{n,0}$. Values of f on a shifted interval $I_{n,s}$ are recovered by using the same coefficients $c_{n,j}$ on a shifted set of scaling function coefficients

$$f(x) \approx \sum_{j=0}^{p-1} f_{n,j+s} c_{n,j}(x - sh) = \sum_{j=s}^{s+p-1} f_{n,j} c_{n,j-s}(x - sh) \quad \text{for } x \in I_{n,s}. \quad (3.10)$$

We can combine (3.9) and (3.10) into the desired form (3.2), (3.3) by defining

$$\beta(x; p, x_0) = \begin{cases} c_{0,p-1}(x + p - 1; p) & \text{if } x \in [x_0 - p + 1, x_0 - p + 2), \\ \vdots \\ c_{0,1}(x + 1; p) & \text{if } x \in [x_0 - 1, x_0), \\ c_{0,0}(x; p) & \text{if } x \in [x_0, x_0 + 1). \end{cases} \quad (3.11)$$

By construction, each $\beta(x; p, x_0)$ is a piecewise polynomial of degree $p-1$ with support $[x_0 - p + 1, x_0 + 1)$ (see figure 1).

Figure 1 goes near here

Formulas for reconstructing the derivatives of f can be obtained by an analogous construction. We use the notation $\beta^{[r]}$ for the function used to reconstruct values of the r th derivative. $f^{(r)}$ denotes the r th derivative of f .

We again start by looking for coefficients $c_{n,j}^{[r]}$ so that

$$f^{(r)}(x) = \sum_{j=0}^{p-1} f_{n,j} c_{n,j}^{[r]}(x) \quad \text{for } f(x) = x^k, k = 0, \dots, p-1.$$

This leads to the matrix equation

$$\mathbf{H}_n \mathbf{M} \mathbf{c}_n^{[r]}(x) = \mathbf{p}^{(r)}(x),$$

from which we easily obtain

$$\mathbf{c}_n^{[r]}(x) = h^{-r} \mathbf{c}_n^{(r)}(x),$$

and therefore

$$\beta^{[r]}(x; p, x_0) = \begin{cases} c_{0,p-1}^{(r)}(x+p-1; p) & \text{if } x \in [x_0 - p + 1, x_0 - p + 2), \\ \vdots \\ c_{0,1}^{(r)}(x+1; p) & \text{if } x \in [x_0 - 1, x_0), \\ c_{0,0}^{(r)}(x; p) & \text{if } x \in [x_0, x_0 + 1). \end{cases} \quad (3.12)$$

Thus,

$$\beta^{[r]}(x; p, x_0) = \beta^{(r)}(x; p, x_0)$$

in the sense of $\beta^{[r]}$ being the r th derivative from the right of β , i.e. ignoring possible discontinuities at the knots $(x_0 + j)$, $j \in \mathbb{Z}$. $\beta^{[r]}$ is therefore a piecewise polynomial of degree $(p - r - 1)$.

REMARKS:

1. It is well-known that Vandermonde matrices have condition numbers which increase rapidly with the size of the matrix. We were not able to avoid this phenomenon by alternative approaches to the derivation of β .

However, β functions for larger p do not appear to offer any real advantages over lower order ones. The lower order functions ($p = 3$ or 4) already give excellent reconstruction results. Some of the higher order functions are oscillatory and thus unsuitable, because of cancellation problems during the reconstruction. The others look very similar to β functions for smaller p (see figure 4), but require a wider support.

For small values of p , we observed no difficulties in the numerical calculation of the coefficients. Even for $p = 10$, we obtained the coefficients of the polynomials $c_{n,j}$ to 10 decimals of accuracy, using the Björck-Pereyra algorithm [1] in 15-decimal arithmetic.

2. If the dual scaling function $\tilde{\phi}$ is a spline, does β equal $\tilde{\phi}$? The answer is: possibly yes, but usually not.

Assume that for some integer p , $\tilde{\phi}$ is a piecewise polynomial of degree $p - 1$, has support of length p and can be used to reconstruct all polynomials up to order $p - 1$. These conditions are satisfied if $\tilde{\phi}$ is the B-spline of order p , for example.

Then, if we use the same p , and if we choose x_0 so that the supports of β and $\tilde{\phi}$ match, the polynomial pieces of both β and $\tilde{\phi}$ satisfy (3.8), and by uniqueness $\tilde{\phi}$ must equal β . For any other choice of p or x_0 , β will be different from $\tilde{\phi}$.

Figure 3 shows the dual scaling function $\tilde{\phi}$ and $\beta(x; p)$ for $p = 2, 3, 4$, for the Daubechies-Cohen spline wavelet with $(N, \tilde{N}) = (3, 3)$. $\beta(x; 3)$ is equal to $\tilde{\phi}$ if we choose $x_0 = 1$, which makes β continuous. $\beta(x; 2)$ and $\beta(x; 4)$ are different from $\tilde{\phi}$, and so is $\beta(x; 3)$ for other choices of x_0 .

3. A natural question to ask is whether β or $\beta^{[r]}$ satisfy recursion relations analogous to (2.1). This is not the case in general, as can be verified from the examples in section 6.

4. We have not used any special properties of ϕ other than $\mathcal{M}_0 = \int \phi(x) dx \neq 0$. Our construction is valid in any setting where data of the form $\langle f, \phi_{n,j} \rangle$ are given.

5. We will discuss the choice of x_0 below. At this point we would just like to point out that it is not required to choose the same x_0 for β and $\beta^{[r]}$. If x_0 and $x_0^{[r]}$ are chosen differently, $\beta^{[r]}$ will be different from $\beta^{(r)}$ (see figure 2, (c), (d)). \square

4. ERROR ESTIMATES

Fix p and x_0 . For $x \in I = [x_0, x_0 + 1)$, the pointwise reconstruction error for the monomial x^k at resolution $h = 2^0$ is

$$e_k(x) = x^k - \sum_{j=0}^{p-1} \langle x^k, \phi_{0,j} \rangle c_{0,j}(x) = x^k - \sum_{j=0}^{p-1} \mathcal{M}_{k,j} c_{0,j}(x).$$

By (3.8), $e_k \equiv 0$ for $k = 0, \dots, p-1$. For $k \geq p$, e_k is a polynomial of degree k .

If $f \in C^p$, then for $x \in I_{n,0}$,

$$f(x) = \sum_{j=0}^{p-1} \frac{f^{(j)}(0)}{j!} x^j + \frac{f^{(p)}(\xi)}{p!} x^p \quad \text{for some } \xi \in I_{n,0}.$$

The reconstruction error for f at the point x is

$$\begin{aligned} f(x) - \sum_{j=0}^{p-1} \langle f, \phi_{n,j} \rangle c_{n,j}(x) &= \sum_{j=0}^{p-1} \frac{f^{(j)}(0)}{j!} h^j e_j(x/h) + \frac{f^{(p)}(\xi)}{p!} h^p e_p(x/h) \quad \text{for some } \xi \in I_{n,0} \\ &= O(h^p), \end{aligned} \tag{4.1}$$

since $f^{(p)}$ and e_p are continuous in $I_{n,0}$.

For $x \in I_{n,s}$ we obtain a corresponding result using Taylor series expansion around the point sh .

If $f \in C^{p+1}$, we can take the Taylor series expansion one step further: For $x \in I_{n,s}$,

$$f(x) - \sum_{j=0}^{p-1} f_{n,j} c_{n,j}(x) = \frac{f^{(p)}(sh)}{p!} h^p e_p((x/h) - s) + O(h^{p+1}). \tag{4.2}$$

If σ is a zero of e_p inside I , the local error at the scaled and translated points $(\sigma + s)h$ is $O(h^{p+1})$.

REMARKS: 1. It is conceivable that the term $O(h^{p+1})$ in (4.2) could also vanish at the same point σ , but that requires specific relationships between the higher moments of ϕ . Unless we are in a position to prescribe the moments of ϕ , we would not expect that to happen.

2. Let σ_k , $k = 1, 2, \dots$ denote the real zeros of e_p . At these points, we *potentially* get higher order accuracy, but only if σ_k lies inside $I = [x_0, x_0 + 1)$. See the numerical examples in section 6 for illustration.

3. It is possible to estimate the error at the point $x \in I_{n,s}$ based on Taylor series expansions around a point different from sh , for example around x itself. Such attempts lead back to the same results presented here, after laborious calculation. \square

Differentiation commutes with all the operations leading to the error estimates (4.1) and (4.2). In particular if $f \in C^p$ and $r < p$, then for $x \in I_{n,0}$

$$\begin{aligned} f^{(r)}(x) &= \sum_{j=0}^{p-r-1} \frac{f^{(j+r)}(0)}{j!} x^j + \frac{f^{(p)}(\xi)}{(p-r)!} x^{p-r} \quad \text{for some } \xi \in I_{n,0} \\ &= \sum_{j=0}^{p-1} \frac{f^{(j)}(0)}{j!} \frac{d^r}{dx^r} x^j + O(h^{p-r}), \\ f_{n,j} &= \sum_{i=0}^{p-1} \frac{f^{(i)}(0)}{i!} h^{i+(1/2)} \mathcal{M}_{i,j} + O(h^{p+(1/2)}) \quad \text{as before,} \\ c_{n,j}^{[r]} &= h^{-r} \frac{d^r}{dx^r} c_{n,j}(x), \end{aligned}$$

which leads to an error estimate at $x \in I_{n,s}$ of

$$\begin{aligned} f^{(r)}(x) - \sum_{j=0}^{p-1} f_{n,j} c_{n,j}^{[r]}(x) &= \sum_{j=0}^{p-1} \frac{f^{(j)}(sh)}{j!} \frac{d^r}{dx^r} [h^j e_j((x/h) - s)] \\ &\quad + \frac{f^{(p)}(sh)}{p!} \frac{d^r}{dx^r} [h^p e_p((x/h) - s)] + O(h^{p-r+1}) \\ &= O(h^{p-r}). \end{aligned} \tag{4.3}$$

Again, the order of convergence is one level higher at certain points. These points $\sigma_k^{[r]}$ are the zeros of $e_p^{[r]}$ in $I_{n,s}$, and are in general different from σ_k .

5. SMOOTHNESS PROPERTIES OF THE β FUNCTIONS

In sections 3 and 4, we had to perform the calculations for an arbitrary level n in order to obtain the correct powers of h . Since smoothness is independent of scaling, it suffices to take $n = 0$, $h = 2^0$ in this section, and we use the notation c_j instead of $c_{0,j}$.

Theorem 5.1. *The function $\beta^{[r]}(x; x_0)$ is continuous everywhere if it is continuous at one of the endpoints of its support.*

Proof. We will write out the proof for $r = 0$. As in the derivation of (4.3), the general proof is then obtained by differentiating everything, since differentiation commutes with all operations we use.

Continuity of β means (see (3.11) and figure 1)

$$\begin{aligned} 0 &= c_0(x_0 + 1), \\ c_j(x_0) &= c_{j+1}(x_0 + 1), \quad j = 0, \dots, p-2 \\ c_{p-1}(x_0) &= 0. \end{aligned}$$

Without loss of generality, assume continuity at the left endpoint, that is $c_{p-1}(x_0) = 0$. Since \mathbf{M} is nonsingular, it suffices to prove

$$\mathbf{M} \begin{pmatrix} 0 \\ c_0(x_0) \\ \vdots \\ c_{p-2}(x_0) \end{pmatrix} = \mathbf{M} \begin{pmatrix} c_0(x_0 + 1) \\ c_1(x_0 + 1) \\ \vdots \\ c_{p-1}(x_0 + 1) \end{pmatrix}$$

The k th entry on the right-hand side is $(x_0 + 1)^k$ by (3.8). Using (2.6), the k th entry on the left is

$$\begin{aligned} \sum_{j=0}^{p-2} \mathcal{M}_{k,j+1} c_j(x_0) &= \sum_{j=0}^{p-1} \mathcal{M}_{k,j+1} c_j(x_0) \quad (\text{since } c_{p-1}(x_0) = 0) \\ &= \sum_{j=0}^{p-1} \left\{ \sum_{\ell=0}^k \binom{k}{\ell} \mathcal{M}_{\ell,j} \right\} c_j(x_0) = \sum_{\ell=0}^k \binom{k}{\ell} x_0^\ell = (x_0 + 1)^k. \end{aligned}$$

□

For even p , c_{p-1} is a polynomial of odd degree, so there always exists a choice of x_0 which makes β continuous. It is not obvious whether that is always possible for odd p , but we were able to find such x_0 in all the examples we considered.

As illustrated in the numerical examples below, $x_0^{[r]}$ should be chosen so that the leading error term $e_p^{[r]}$ is small over the interval $[x_0^{[r]}, x_0^{[r]} + 1)$, whether or not this makes $\beta^{[r]}$ continuous. However, in all examples we tried we were able to find $x_0^{[r]}$ which produces a continuous $\beta^{[r]}$ and small error simultaneously.

The following lemma, together with theorem 5.1, states that the starting points $x_0^{[r]}$ which make $\beta^{[r]}(x; p+1)$ continuous are the same as the points $\sigma^{[r]}$ of (potentially) higher accuracy for $\beta^{[r]}(x; p)$.

Lemma 5.2. *For any $r < p$, if $c_p^{[r]}(\sigma; p+1) = 0$, then*

$$c_j^{[r]}(\sigma; p+1) = c_j^{[r]}(\sigma; p), \quad j = 0, \dots, p-1, \quad (5.1)$$

and

$$e_p^{[r]}(\sigma) = \frac{d^r}{d\sigma^r} \sigma^p - \sum_{j=0}^{p-1} \mathcal{M}_{p,j} c_j^{[r]}(\sigma; p) = 0. \quad (5.2)$$

Proof. We will show the proof for $r = 0$ only; the proof for general r proceeds along identical lines, with derivatives inserted all over the place.

Assume $c_p(\sigma; p+1) = 0$, then

$$\mathbf{M}(p+1)\mathbf{c}(\sigma; p+1) = \left(\begin{array}{ccc|c} & & & \mathcal{M}_{0,p} \\ & & & \vdots \\ & & & \mathcal{M}_{p-1,p} \\ \hline \mathbf{M}(p) & & & \mathcal{M}_{p,p} \end{array} \right) \begin{pmatrix} c_0(\sigma; p+1) \\ \vdots \\ c_{p-1}(\sigma; p+1) \\ 0 \end{pmatrix} = \begin{pmatrix} \sigma^0 \\ \vdots \\ \sigma^{p-1} \\ \sigma^p \end{pmatrix} \quad (5.3)$$

Thus,

$$\mathbf{M}(p) \begin{pmatrix} c_0(\sigma; p+1) \\ \vdots \\ c_{p-1}(\sigma; p+1) \end{pmatrix} = \begin{pmatrix} \sigma^0 \\ \vdots \\ \sigma^{p-1} \end{pmatrix}$$

which implies (5.1) by uniqueness of the solution of (3.8).

Eq. (5.2) is the last equation in (5.3), using (5.1). □

We summarize the results of the last three sections in the following theorem:

Theorem 5.3. *For any choice of ϕ , p , $r < p$, $x_0^{[r]}$, there exists a function $\beta^{[r]}(x) = \beta^{[r]}(x; \phi, p, x_0^{[r]})$ so that for $f \in C^p$ and for any $x \in \mathbb{R}$,*

$$|f^{(r)}(x) - B_n^{[r]}f(x)| = O(h^{p-r}),$$

where

$$\begin{aligned} h &= 2^{-n}, \\ B_n^{[r]}f &= \sum_{j=-\infty}^{\infty} f_{n,j} \beta_{n,j}^{[r]}, \\ \beta_{n,j}^{[r]}(x) &= 2^{n/2} \beta^{[r]}(2^n x - j). \end{aligned}$$

$\beta^{[r]}(x; \phi, p, x_0^{[r]})$ has support $[x_0^{[r]} - p + 1, x_0^{[r]} + 1]$ and is a polynomial of degree at most $p - r - 1$ on each subinterval $[x_0^{[r]} + j, x_0^{[r]} + j + 1]$, $j \in \mathbb{Z}$.

For $f \in C^{p+1}$ and $x \in [(x_0^{[r]} + s)/h, (x_0^{[r]} + s + 1)/h]$, the error is given by

$$|f^{(r)}(x) - B_n^{[r]}f(x)| = \frac{f^{(p)}(sh)}{p!} h^{p-r} e_p^{(r)}((x/h) - s) + O(h^{p-r+1}). \tag{5.4}$$

If $\sigma^{[r]}$ is a real zero of $e_p^{(r)}$ in $[x_0^{[r]}, x_0^{[r]} + 1)$, then

$$|f^{(r)}((\sigma^{[r]} + s)h) - B_n^{[r]}f((\sigma^{[r]} + s)h)| = O(h^{p-r+1}), \quad s \in \mathbb{Z}.$$

6. NUMERICAL EXAMPLES

6.1. Examples of β Functions. For small values of p , we can do most calculations in closed form. The calculations really depend only on the moments of ϕ , not on ϕ itself.

For $p = 2$,

$$\begin{aligned} \mathbf{M} &= \begin{pmatrix} 1 & 1 \\ \mathcal{M}_1 & \mathcal{M}_1 + 1 \end{pmatrix} \\ c_0(x) &= (\mathcal{M}_1 + 1) - x \\ c_1(x) &= -\mathcal{M}_1 + x \end{aligned}$$

β is continuous if $x_0 = \mathcal{M}_1$; with this choice of x_0 , β is a ‘‘hat function’’. The points σ of potentially higher accuracy are the solutions of

$$e_2(\sigma) = \sigma^2 - \mathcal{M}_{2,0}c_0(\sigma) - \mathcal{M}_{2,1}c_1(\sigma) = 0,$$

which leads to

$$\sigma = \frac{1}{2} \left(2\mathcal{M}_1 + 1 \pm \sqrt{4\mathcal{M}_2 - 4\mathcal{M}_1^2 + 1} \right).$$

If $\mathcal{M}_2 = \mathcal{M}_1^2$, which happens for all orthogonal wavelets with at least 2 vanishing moments, then $\sigma = \mathcal{M}_1$ or $\mathcal{M}_1 + 1$.

$\beta^{[1]}$ is always a step function and is never continuous. The leading error term for $B_n^{[1]}$ vanishes if

$$e_2'(\sigma^{[1]}) = 2\sigma^{[1]} - \mathcal{M}_{2,0}c_0'(\sigma^{[1]}) - \mathcal{M}_{2,1}c_1'(\sigma^{[1]}) = 0,$$

which leads to

$$\sigma^{[1]} = \mathcal{M}_1 + \frac{1}{2}.$$

For $p = 3$, β is continuous if

$$x_0 = \frac{1}{2} \left(2\mathcal{M}_1 + 1 \pm \sqrt{4\mathcal{M}_2 - 4\mathcal{M}_1^2 + 1} \right),$$

and $\beta^{[1]}$ is continuous if

$$x_0^{[1]} = \mathcal{M}_1 + \frac{1}{2}.$$

These are the σ , $\sigma^{[1]}$ for $p = 2$ (see remark after lemma 5.2). $\beta^{[2]}$ is always a step function and is never continuous.

The leading error term for B_n vanishes if

$$e_3(\sigma) = \sigma^3 - \mathcal{M}_{3,0}c_0(\sigma) - \mathcal{M}_{3,1}c_1(\sigma) - \mathcal{M}_{3,2}c_2(\sigma) = 0.$$

The resulting cubic equation cannot be solved in closed form in general. If $\mathcal{M}_2 = \mathcal{M}_1^2$, $\mathcal{M}_3 = \mathcal{M}_1^3$, which happens in the case of higher order coiflets, then $\sigma = \mathcal{M}_1$, $\mathcal{M}_1 + 1$ or $\mathcal{M}_1 + 2$.

The leading error term for $B_n^{[1]}$ vanishes for

$$\sigma^{[1]} = 1 + \mathcal{M}_1 \pm \sqrt{1/3 - \mathcal{M}_1^2 + \mathcal{M}_2}.$$

The leading error term for $B_n^{[2]}$ vanishes for

$$\sigma^{[2]} = 1 + \mathcal{M}_1.$$

As particular examples, we consider two types of wavelets:

- The orthogonal Daubechies wavelet with 2 vanishing moments ([3], p. 194 ff.). Its first few moments are

$$\mathcal{M}_0 = 1, \quad \mathcal{M}_1 = (3 - \sqrt{3})/2 \approx 0.633975, \quad \mathcal{M}_2 = 3(2 - \sqrt{3})/2 \approx 0.40192.$$

- The biorthogonal Daubechies-Cohen spline wavelet with $(N, \tilde{N}) = (3, 3)$ (see [2], page 543, or [3], page 271 ff.). Its first few moments are

$$\mathcal{M}_0 = 1, \quad \mathcal{M}_1 = 1/2, \quad \mathcal{M}_2 = 0, \quad \mathcal{M}_3 = -1/4,$$

The points $x_0^{[r]}$ and $\sigma^{[r]}$ for $p = 2$ and 3 are summarized in table 1. The dual scaling functions and some of the functions β , $\beta^{[1]}$ are shown in figures 2, 3, and 4.

Table 1 goes near here

Figures 2, 3 and 4 go near here

6.2. Reconstruction Examples. The numerical examples were done on a DECstation 5000/133, using Matlab 4.2c. The scaling function coefficients $f_{n,j}$ were calculated numerically to accuracy 10^{-12} , all subsequent calculations were done by Matlab in double precision.

Most of the examples are based on the reconstruction of the function $f(x) = \sin x$ on the interval $[0, 3]$.

First, we illustrate the error estimates (4.1) through (4.3), using the Daubechies wavelet with 2 vanishing moments and accuracy level $p = 3$.

The underlined values in table 2 are approximately proportional to $f'''(0)h^3$ and decrease by the expected factor of 8 at each level; the values in each row (errors at a fixed point x for different resolutions) are not directly comparable.

Table 2 goes near here

Table 3(a) shows the maximum errors at equally spaced points across the interval $[0, 3]$ for the original scaling function series (1.1) and for continuous β and $\beta^{[1]}$ with $p = 3$. Also shown are the maximum errors at scaled translates of σ_k .

As expected, for general points the ratio of errors at different resolutions approaches 4 for ϕ and $\beta^{[1]}$, and 8 for β . This indicates errors of order $O(h^2)$ and $O(h^3)$, respectively.

For the points σ_1 and σ_2 , which are inside I , convergence is of order $O(h^4)$. σ_3 lies outside I , and the ratio approaches the value of 8, corresponding to the error $O(h^3)$ valid for general points.

Table 3 goes near here

Figure 5 shows the reconstructions themselves, at resolution $h = 2^0$. Figure 6 compares the reconstruction errors for ϕ and for β , as well as the error at scaled translates of σ_1 , at resolution $h = 2^{-4}$; note the logarithmic scale on the vertical axis.

Figures 5 and 6 go near here

Second, we illustrate the effect of the choice of x_0 .

Part (b) of table 3 is comparable to the first two lines of part (a), except that we have chosen $x_0 = 0$. For this choice, β is not continuous (see figure 2(e)). The errors still decay at the expected rate, but they are now much larger.

To understand the influence of x_0 better, consider the graph of e_3 in figure 7. The error depends on the size of e_3 over the interval $I = [x_0, x_0 + 1)$. In general, we would expect e_3 to be small if I is located somewhere in the region between the zeros of e_3 (such as $x_0 = 1.633975$), larger if I is farther away from the region of zeros (such as $x_0 = 0$).

The size of the error does not depend on whether β is continuous or not, but it is esthetically more pleasing to have a continuous approximating function if an x_0 can be found in the region where e_p is small.

Figure 7 goes near here

Third, we demonstrate that our results work equally well for biorthogonal wavelets.

Part (c) of table 3 shows results comparable to the first two lines of part (a), for the biorthogonal Daubechies-Cohen spline wavelet with $(N, \tilde{N}) = (4, 2)$ (see [3], p.271 ff). In this case, our reconstruction is less accurate, but faster, than the scaling function series.

Experiments with other wavelets and with other smooth and slowly varying functions yield similar results to the ones presented so far.

Finally, figures 8 and 9 illustrate what happens in the case of a highly oscillating function; results for functions with singularities are similar.

As shown in figure 8, the reconstruction $B_n f$ is smoother looking, but not any closer to the original curve than the scaling function series $\tilde{P}_n f$. However, the accuracy of $B_n f$ is not any worse than the accuracy of $\tilde{P}_n f$, either.

Figure 9 illustrates that the error at the scaled translates of σ_k is not noticeably smaller than at other points. Obviously, the error in the case of a highly oscillating function is not described all that well by the leading term.

Figures 8 and 9 go near here

7. SUMMARY

For situations where it is desired to recover point values of a function f to high accuracy from its scaling function coefficients $f_{n,j}$, we propose to replace the standard scaling function series

$$\tilde{P}_n f = \sum_{j=-\infty}^{\infty} \langle f, \phi_{n,j} \rangle \tilde{\phi}_{n,j}$$

by a corresponding series

$$B_n f = \sum_{j=-\infty}^{\infty} \langle f, \phi_{n,j} \rangle \beta_{n,j},$$

or more generally

$$f^{(r)}(x) \approx B_n^{[r]} f = \sum_{j=-\infty}^{\infty} \langle f, \phi_{n,j} \rangle \beta_{n,j}^{[r]}.$$

Theoretical estimates and numerical experiments indicate that the new series $B_n f$ has accuracy at least as good as the scaling function series for all functions f , and performs significantly better for smooth, slowly varying f .

In addition, derivatives of f can be recovered by using the related series $B_n^{[r]} f$, for which there is in general no counterpart using derivatives of scaling functions.

8. ACKNOWLEDGMENTS

The authors would like to thank the (anonymous) referee for many helpful hints which led to improved clarity and simplified proofs.

REFERENCES

- [1] Å. Björck and V. Pereyra, Solution of Vandermonde systems of equations, *Math. Comp.* **24** (1970), 893–903.
- [2] A. Cohen, I. Daubechies, and J.-C. Feauveau, Biorthogonal bases of compactly supported wavelets, *Comm. Pure Appl. Math.* **45** (1992), 485–560.
- [3] I. Daubechies, “Ten Lectures on Wavelets”, vol. 61 of CBMS-NSF Regional Conference Series in Applied Mathematics, SIAM, Philadelphia, 1992.
- [4] S. Kelly, M. Kon, and L. Raphael, Pointwise convergence of wavelet expansions, *Bull. Amer. Math. Soc.* **30** (1994), 87–94.
- [5] S. G. Mallat, Multiresolution approximations and wavelet orthonormal bases of $L^2(\mathbb{R})$, *Trans. Amer. Math. Soc.* **315** (1989), 69–87.
- [6] W. Sweldens and R. Piessens, Quadrature formulae and asymptotic error expansions for wavelet approximations of smooth functions, *SIAM J. Numer. Anal.* **31** (1994), 1240–1264.

- [7] G. G. Walter, "Wavelets and Other Orthogonal Systems with Applications", CRC Press, Boca Raton, 1994.

TABLE 1. Choices of starting points $x_0^{[r]}$ which make $\beta^{[r]}$ continuous, and points $\sigma^{[r]}$ of potentially higher accuracy, for (a) orthogonal Daubechies wavelet with 2 vanishing moments (b) biorthogonal Daubechies-Cohen spline wavelet with $(N, \tilde{N}) = (3, 3)$.

		(a)		(b)	
		$x_0^{[r]}$	$\sigma^{[r]}$	$x_0^{[r]}$	$\sigma^{[r]}$
$p = 2$	$r = 0$	$(3 - \sqrt{3})/2$	$(3 - \sqrt{3})/2$ $(5 - \sqrt{3})/2$	$1/2$	1
	$r = 1$		$(4 - \sqrt{3})/2$		1
$p = 3$	$r = 0$	$(3 - \sqrt{3})/2$	0.57706	1	1
		$(5 - \sqrt{3})/2$	1.75968		$3/2$
			2.56518		2
	$r = 1$	$(4 - \sqrt{3})/2$	$(5 - \sqrt{3})/2 + 1/\sqrt{3}$ $(5 - \sqrt{3})/2 - 1/\sqrt{3}$	1	$(9 + \sqrt{3})/6$ $(9 - \sqrt{3})/6$
$r = 2$		$(5 - \sqrt{3})/2$		1	

TABLE 2. Comparison of errors at several points x and several resolutions h , for reconstruction of $\sin x$ using $\beta(x; p = 3, x_0 = 1.633975)$, based on Daubechies wavelet with 2 vanishing moments. The underlined values show the predicted convergence behavior $O(h^3)$.

x	$h = 2^0$	$h = 2^{-1}$	$h = 2^{-2}$
0.25	0.0020729566	0.0005046129	<u>0.0000621160</u>
...			
0.50	0.0040526588	<u>0.0004775991</u>	0.0000575524
...			
1.00	<u>0.0031835356</u>	0.0003380129	0.0000381963

TABLE 3. Comparison of maximum errors at various resolutions, for reconstruction of $\sin x$ or its derivative on $[0, 3]$. The errors were calculated either at equally spaced points with spacing Δx , or at all scaled and translated versions of the points σ_i . The second part of the table shows ratios between adjacent columns in the first part. (a) Using continuous $\beta(x; p = 3, x_0 = 1.633975)$ and $\beta^{[1]}(x; p = 3, x_0 = 1.133975)$ based on Daubechies wavelet with 2 vanishing moments. (b) Using discontinuous $\beta(x; p = 3, x_0 = 0)$ based on Daubechies wavelet with 2 vanishing moments. (c) Using continuous $\beta^{[1]}(x; p = 3, x_0 = 1.133975)$ based on the biorthogonal Daubechies-Cohen spline wavelet with $(N, \tilde{N}) = (3, 3)$.

Maximum errors							
	reconstruction using	errors evaluated for	$h = 2^0$	$h = 2^{-1}$	$h = 2^{-2}$	$h = 2^{-3}$	
(a)	ϕ	$\Delta x = 1/64$	0.2230931	0.0597919	0.0154932	0.0038994	
		β	$\Delta x = 1/64$	0.0418520	0.0054484	0.0006783	0.0000842
	$\beta^{[1]}$	$\sigma_1 = 2.565179$	0.0179483	0.0012485	0.0000801	0.0000050	
		$\sigma_2 = 1.759679$	0.0072115	0.0004933	0.0000316	0.0000020	
		$\sigma_3 = 0.577066$	0.0162341	0.0012062	0.0000898	0.0000079	
	$\Delta x = 1/64$	0.1420792	0.0402152	0.0103265	0.0025981		
(b)	ϕ	$\Delta x = 1/64$	0.2230931	0.0597919	0.0154932	0.0038994	
	β	$\Delta x = 1/64$	0.3933545	0.0531412	0.0067300	0.0008467	
(c)	ϕ	$\Delta x = 1/64$	0.0983246	0.0084478	0.0005585	0.0000354	
	β	$\Delta x = 1/64$	0.0993215	0.0139191	0.0017952	0.0002273	
Ratios							
(a)	ϕ	$\Delta x = 1/64$		3.7311581	3.8592332	3.9732578	
		β	$\Delta x = 1/64$		7.6815296	8.0325838	8.0536774
	$\beta^{[1]}$	$\sigma_1 = 2.565179$			14.3753306	15.5893594	15.9203390
		$\sigma_2 = 1.759679$			14.6201103	15.6096820	15.8281089
		$\sigma_3 = 0.577066$			13.4590785	13.4291017	11.4237320
	$\Delta x = 1/64$			3.5329707	3.8943582	3.9746441	
(b)	ϕ	$\Delta x = 1/64$		3.7311581	3.8592332	3.9732578	
	β	$\Delta x = 1/64$		7.4020651	7.8961797	7.9484083	
(c)	ϕ	$\Delta x = 1/64$		11.6390266	15.1266675	15.7609234	
	β	$\Delta x = 1/64$		7.1356205	7.7535307	7.8987923	

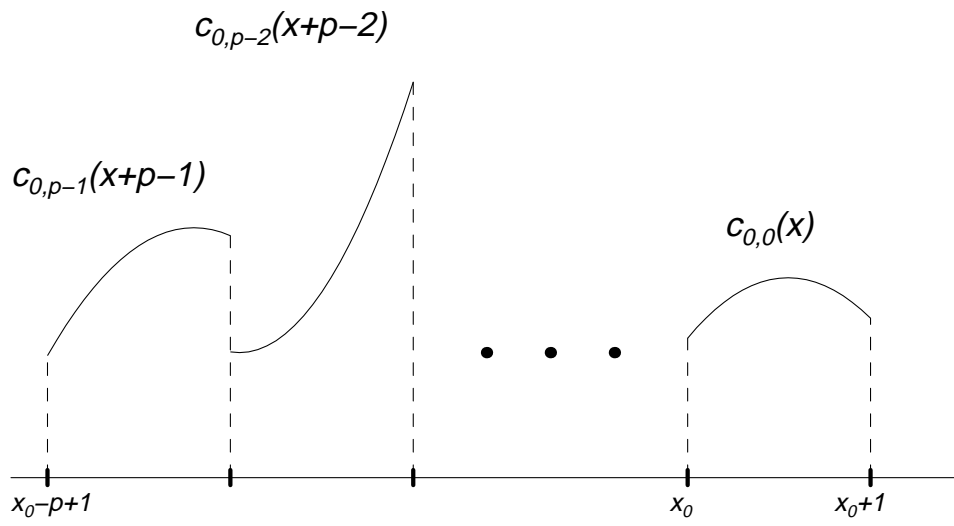
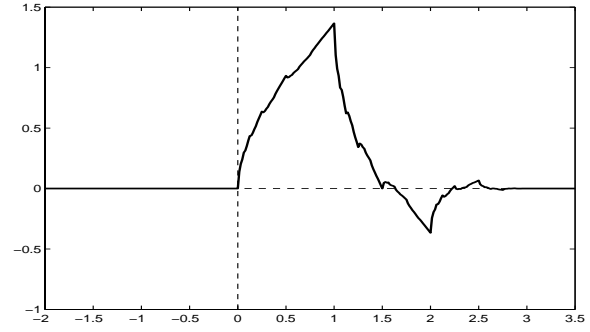
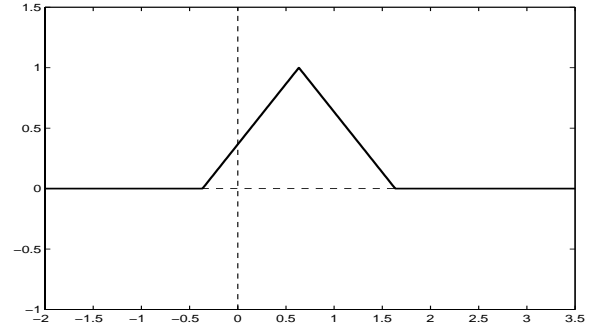
FIGURE 1. Construction of $\beta(x; p, x_0)$ 

FIGURE 2. Examples of $\beta^{[r]}$ for Daubechies Wavelet with 2 Vanishing Moments

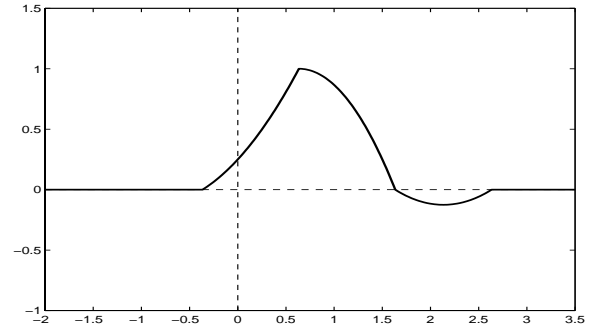
(a) Scaling function ϕ



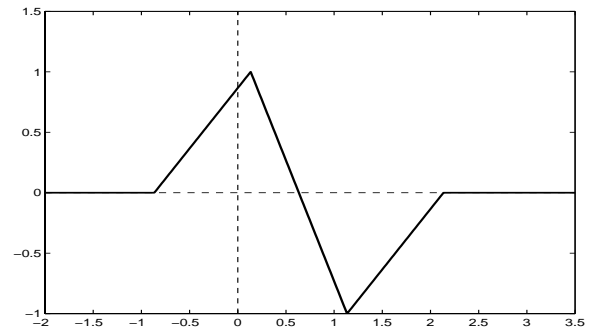
(b) $\beta(x; p = 2, x_0 = \mathcal{M}_1)$



(c) $\beta(x; p = 3, x_0 = \mathcal{M}_1 + 1)$



(d) $\beta^{[1]}(x; p = 3, x_0 = \mathcal{M}_1 + 1/2)$



(e) $\beta(x; p = 3, x_0 = 0)$

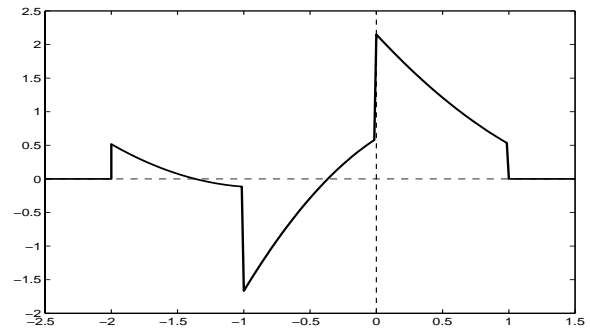
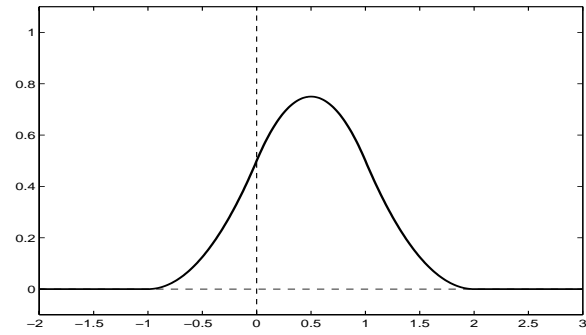
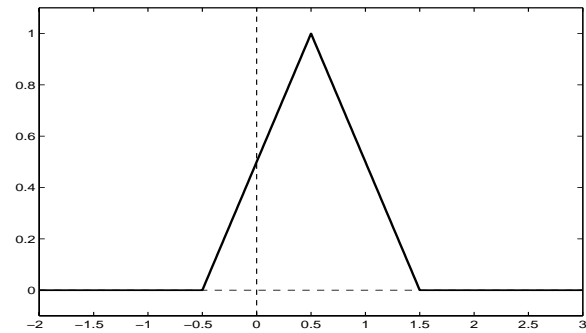


FIGURE 3. Examples of $\beta^{[r]}$ for Biorthogonal Cohen-Daubechies Spline Wavelet with $(N, \tilde{N}) = (3, 3)$

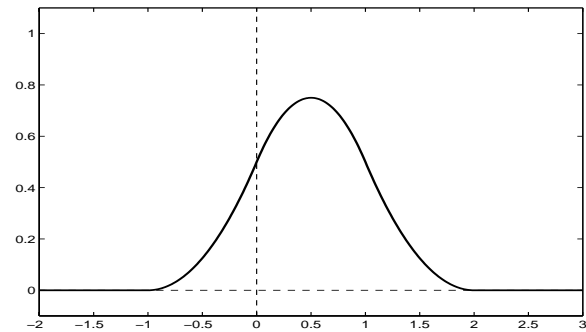
(a) Dual scaling function $\tilde{\phi}$



(b) $\beta(x; p = 2, x_0 = 1/2)$



(c) $\beta(x; p = 3, x_0 = 1)$



(d) $\beta(x; p = 4, x_0 = 3/2)$

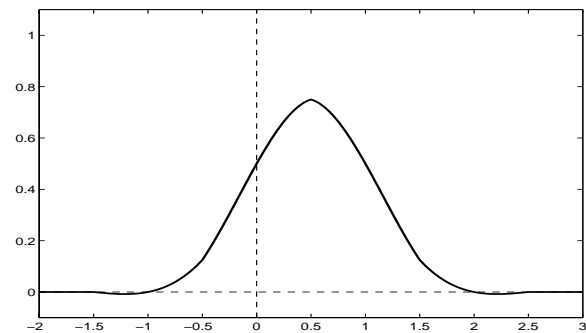
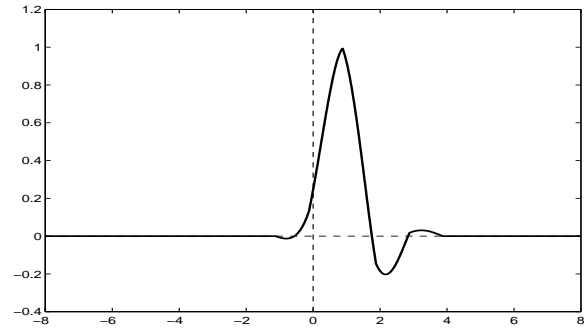
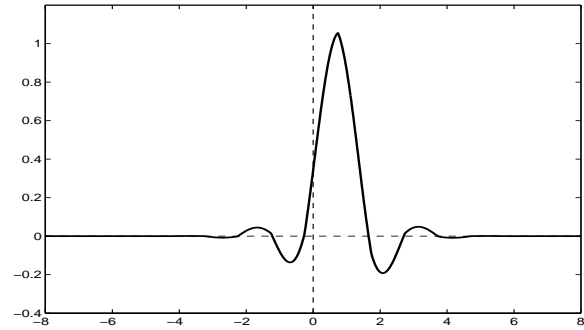


FIGURE 4. β for Large p , for Daubechies Wavelet with 2 Vanishing Moments

(a) $\beta(x; p = 5)$



(b) $\beta(x; p = 10)$



(c) $\beta(x; p = 15)$

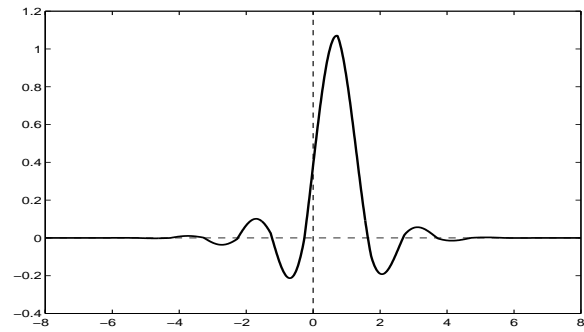


FIGURE 5. Reconstruction of $\sin x$ at resolution $h = 2^0$. Dotted line: original function; dashed line: series using Daubechies wavelet with 2 vanishing moments; solid line: series using $\beta(x; p = 3, x_0 = \mathcal{M}_1 + 1)$.

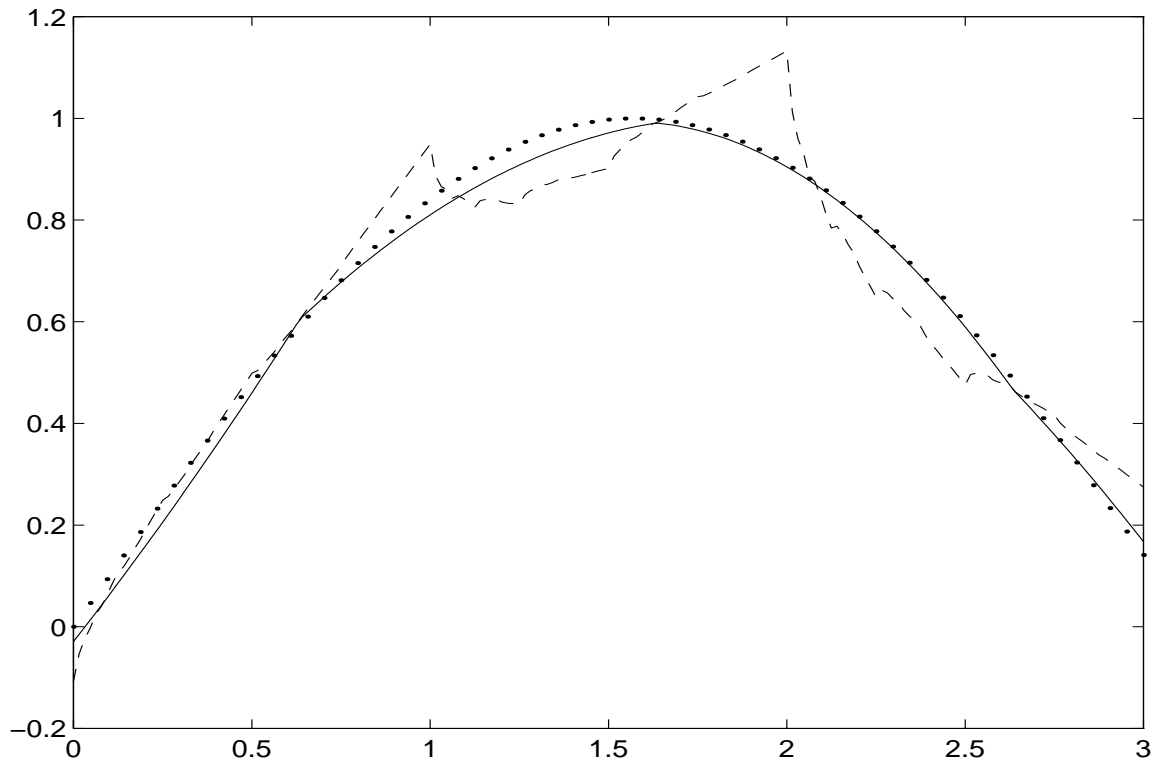


FIGURE 6. Pointwise reconstruction error in reconstruction of $\sin x$ at resolution $h = 2^{-4}$. Dashed line: error using Daubechies wavelet with 2 vanishing moments; solid line: error using $\beta(x; p = 3, x_0 = \mathcal{M}_1 + 1)$; circled points: error at scaled translates of $\sigma_1 \approx 2.56518$.

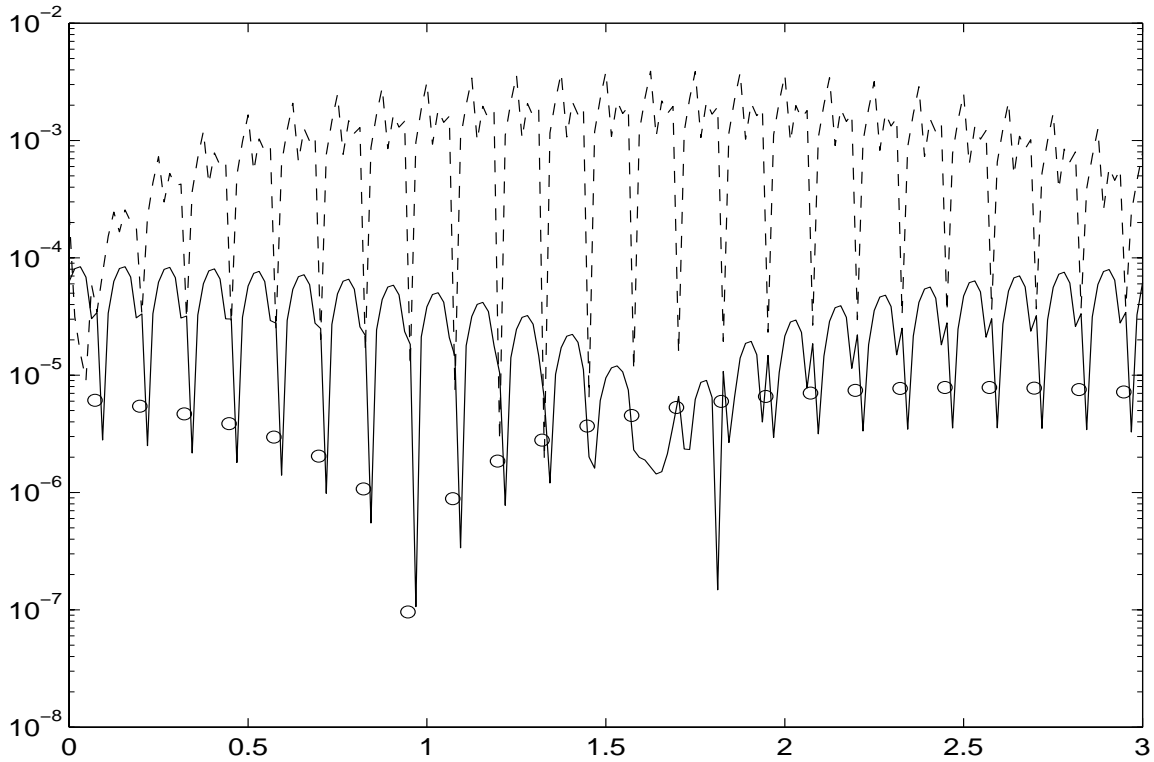


FIGURE 7. Leading error term $e_3(x)$ for $\beta(x; p = 3)$, based on Daubechies wavelet with 2 vanishing moments. Zeros of the function (i.e. points σ_j) are circled.

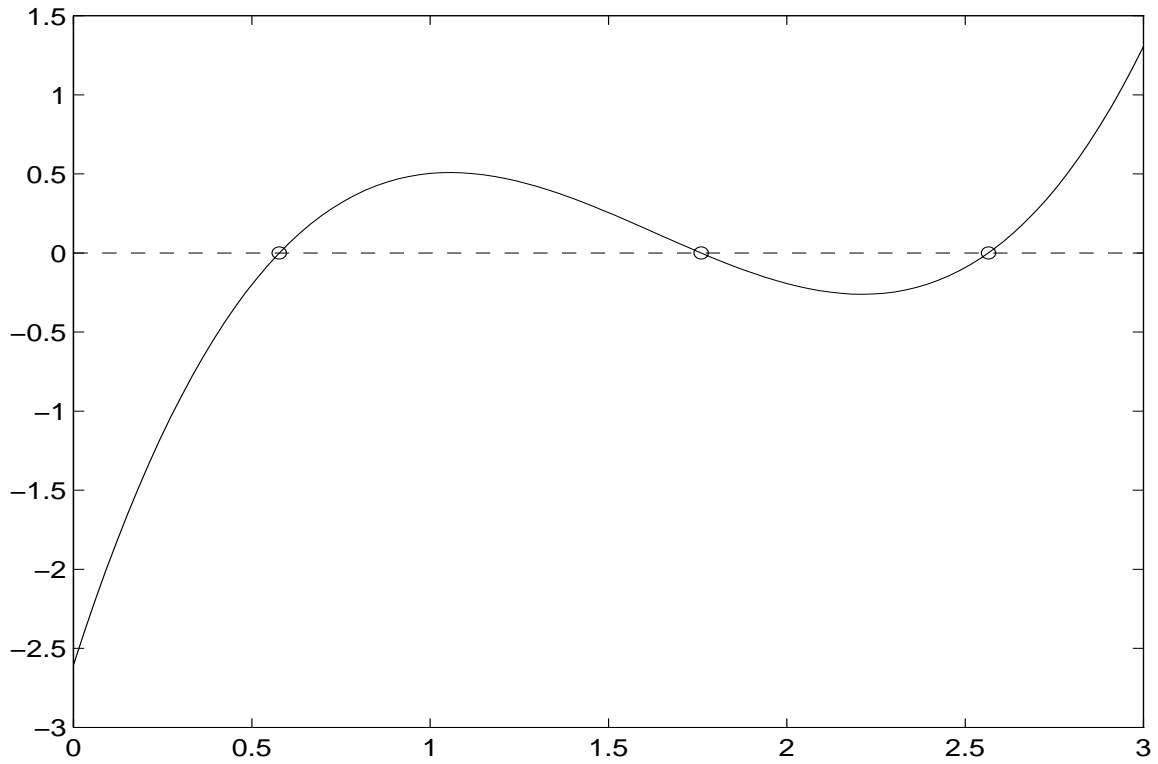


FIGURE 8. Reconstruction of $\sin x + 0.5 \cdot \sin(2.5(x - 1)) + 0.7 \cdot \sin(6(x + 1))$ at resolution $h = 2^0$. Dotted line: original function; dashed line: series using Daubechies wavelet with 2 vanishing moments; solid line: series using $\beta(x; p = 3, x_0 = \mathcal{M}_1 + 1)$.

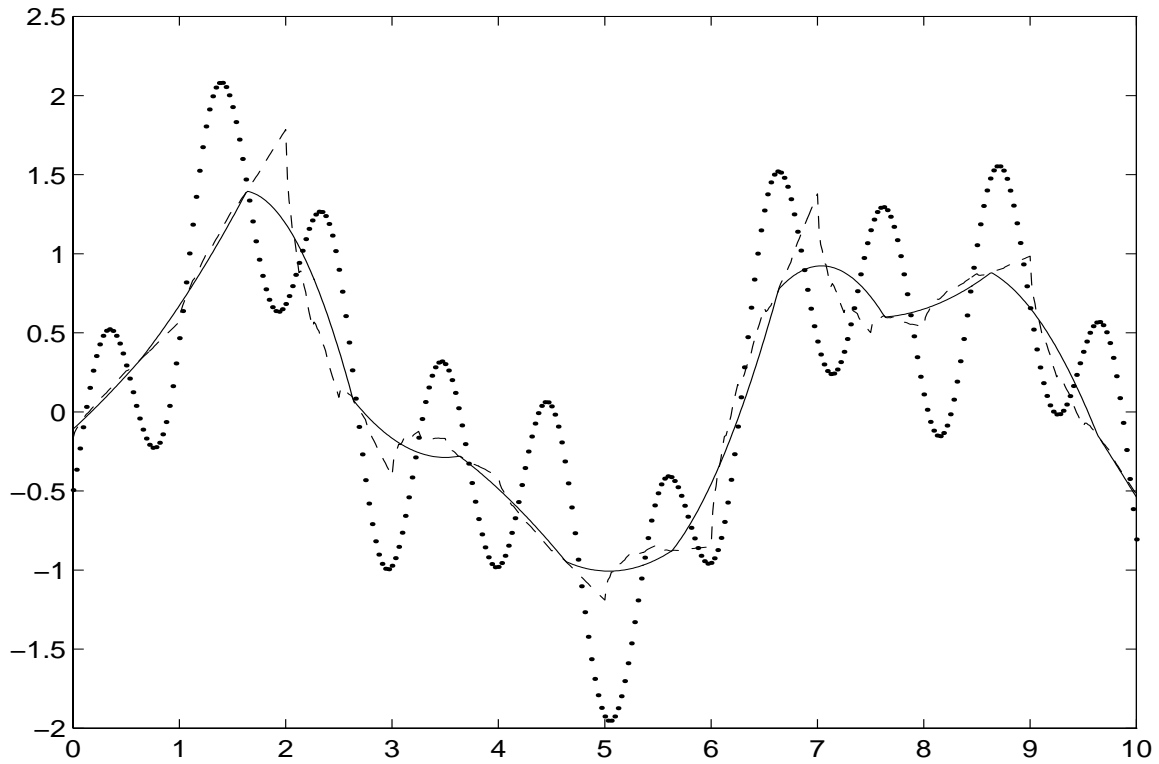
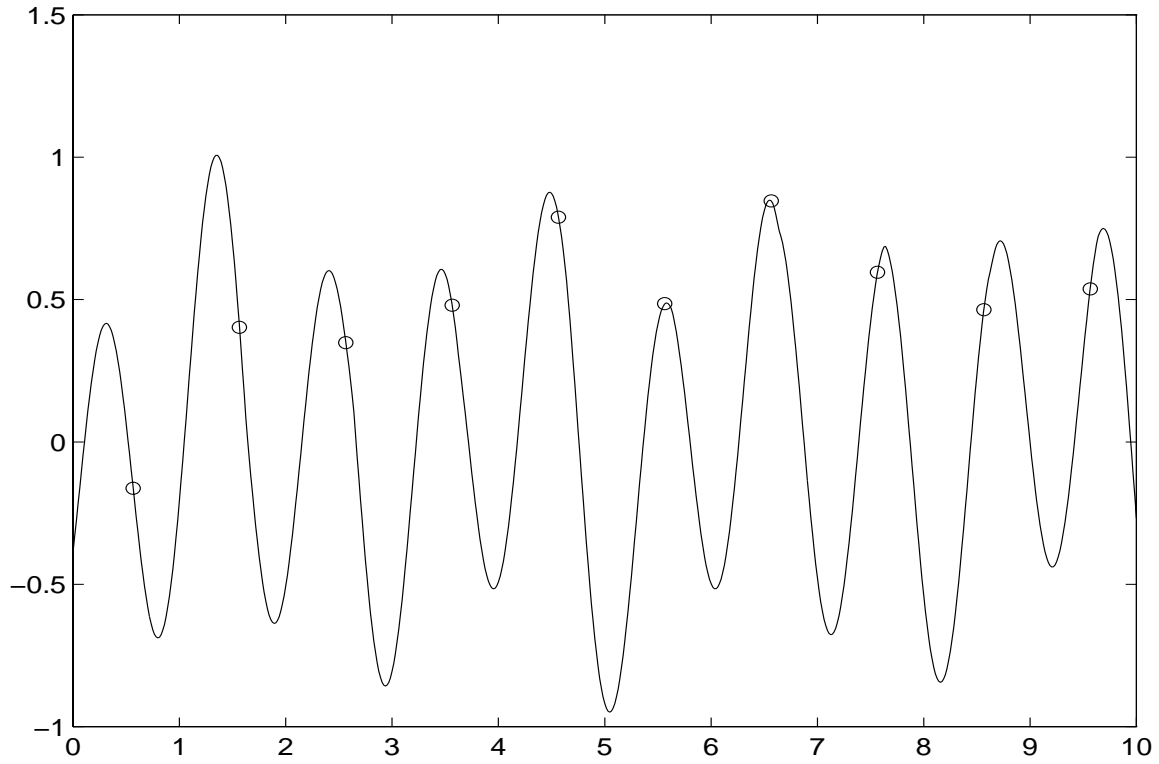


FIGURE 9. Pointwise reconstruction error in reconstruction of $\sin x + 0.5 \cdot \sin(2.5(x - 1)) + 0.7 \cdot \sin(6(x + 1))$ at resolution $h = 2^0$. Solid line: error using $\beta(x; p = 3, x_0 = \mathcal{M}_1 + 1)$; circled points: error at scaled translates of $\sigma_1 \approx 2.56518$.



DEPARTMENT OF MATHEMATICS, IOWA STATE UNIVERSITY, AMES, IA 50011
E-mail address: `keinert@iastate.edu`

DEPARTMENT OF MATHEMATICS, IOWA STATE UNIVERSITY, AMES, IA 50011
E-mail address: `sgkwon@iastate.edu`